Uplift of Africa as a potential cause for Neogene intensification of the Benguela upwelling system

Gerlinde Jung*, Matthias Prange and Michael Schulz

The Benguela Current, located off the west coast of southern Africa, is tied to a highly productive upwelling system[1]. Over the past 12 million years, the current has cooled, and upwelling has intensified[2–4]. These changes have been variously linked to atmospheric and oceanic changes associated with the glaciation of Antarctica and global cooling[5], the closure of the Central American Seaway[1,6] or the further restriction of the Indonesian Seaway[3]. The upwelling intensification also occurred during a period of substantial uplift of the African continent[7,8]. Here we use a coupled ocean–atmosphere general circulation model to test the effect of African uplift on Benguela upwelling. In our simulations, uplift in the East African Rift system and in southern and southwestern Africa induces an intensification of coastal low-level winds, which leads to increased oceanic upwelling of cool subsurface waters. We compare the effect of African uplift with the simulated impact of the Central American Seaway closure[9], Indonesian Throughflow restriction[10] and Antarctic glaciation[11], and find that African uplift has at least an equally strong influence as each of the three other factors. We therefore conclude that African uplift was an important factor in driving the cooling and strengthening of the Benguela Current and coastal upwelling during the late Miocene and Pliocene epochs.

Today, the atmospheric Benguela jet is found at the eastern flank of the subtropical South Atlantic anticyclone just off the coast of southern Africa. This low-level wind maximum is closely connected to the area of maximum oceanic upwelling[12] and is influenced by the land–sea thermal contrast and the presence of a coastal mountain chain. As the thermal land–sea contrast increases with strengthened upwelling, the intensity of upwelling and that of the Benguela jet are connected through a positive feedback[12]. Model-based sensitivity studies for the California jet, which shares common features with the Benguela jet[12], revealed a substantial alteration of jet strength and shape due to coastal topography[13]. For the Benguela region it has also been discussed that the steep slope along the coast leads not only to strengthening, but also a reduced seasonal variability of the wind. This stabilizes the flow and hence favours oceanic upwelling[1].

Southern and eastern African plateaux are considered to form part of the so-called African superswell[14], which was emplaced in the early Miocene[15] and successively lifted during the Neogene[16,17] with phases of major uplift since the late Miocene[7,8]. The exact timing of uplift as well as regional uplift rates and estimates of palaeoelevations, however, remain controversial. For the Namibian dome, a continuous uplift with linearly increasing uplift rates since the late Miocene was estimated whereas the Bié Plateau and the South African dome show maxima in uplift rates in the late Miocene/early Pliocene period[7]. In contrast, another study suggests

negligible Neogene uplift of the South African Plateau[18]. Recently, for East Africa, evidence emerged for a rather simultaneous beginning of uplift of the eastern and western branches around 25 million years ago[19] (Ma), in contrast to a later uplift of the western part around 5 Ma as previously suggested[20]. Palaeoelevation change estimates, for example for the Bié Plateau, during the past 10 Myr range from ~150 m (ref. 16) to 1,000 m (ref. 7). These discrepancies depend strongly on the methods used for the estimation of uplift, some giving more reliable estimates of the timing of uplift than of uplift rates[16], whereas others are better suited for estimating palaeoelevations but less accurate in the timing[7].

Despite these uncertainties, there is evidence for uplift processes that coincide with the two-step development documented for Benguela upwelling intensification at around 12–10 Ma and after 5 Ma (ref. 2). Studies exist that indicate an intensified uplift of the South African dome in the past 10 Myr, of the Bié Plateau from 5 to 2 Ma (refs 7,21), increasing uplift rates during the past 10 Myr for the Namibia dome[7], as well as intensified rifting in the western part of the East African Rift during the late Miocene and at about 4–2 Ma (ref. 22).

A clear intercomparison of uplift history and timing of upwelling intensification is not possible at present, owing to the controversy in timing of uplift and palaeoelevations, but also owing to the much lower temporal resolution of uplift history dating compared with oceanic palaeotemperature and productivity proxy time series. However, considering the possible co-occurrence of uplift and coastal upwelling intensification, we reason that uplift of Africa was a likely factor in driving long-term changes in the Benguela upwelling system.

We test this hypothesis by means of a coupled general circulation model. Although it has been suggested that uplift altered atmosphere and ocean dynamics as well as coastal upwelling in other regions[23], no modelling study has investigated the impact of uplift on the Benguela Current and upwelling system so far.

Our simulations were performed with the Community Climate System Model version 3 (CCSM3; ref. 24). The model simulations do not represent a specific time in Earth history. Instead we carried out a series of sensitivity experiments to give an insight into processes that are important for coastal upwelling intensification due to uplift. Four experiments were performed, a control run with present-day topography (HIGH), a simulation identical to that, except for a lowered eastern and southern African topography to half of the present-day level (LOW), and two additional simulations lowering East (EALOW) and southern African (SALOW) topographies separately (Supplementary Methods).

According to our model simulations, the uplift of southern and eastern Africa leads to a strengthening of the horizontal wind at
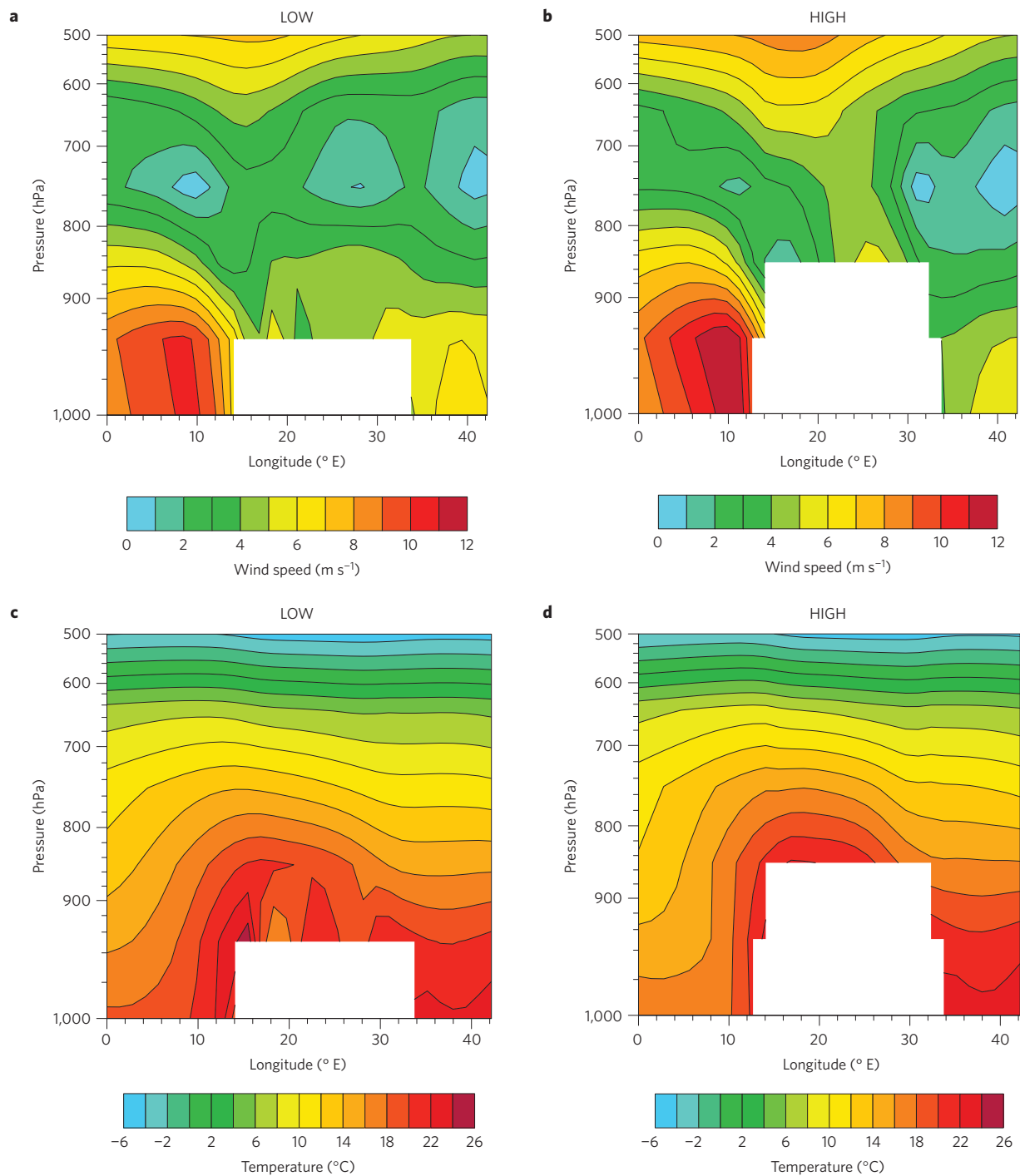
MARUM - Center for Marine Environmental Sciences and Faculty of Geosciences, University of Bremen, 28334 Bremen, Germany.
*e-mail: gjung@marum.de

Figure 1 | Vertical cross-sections at 25° S of annual mean horizontal wind speed (representing the low-level Benguela jet) and air temperature.
a, Horizontal wind speed for low African topography (LOW). **b**, Horizontal wind speed for present-day topography (HIGH). **c**, Temperature for low African topography (LOW). **d**, Temperature for present-day topography (HIGH).

the eastern limb of the subtropical anticyclone with the strongest intensification occurring in the vicinity of the southwest African coast in the region of the Benguela jet. The maximum intensification is seasonally varying in magnitude (around 2.5 m s⁻¹ to more than 4 m s⁻¹) and in location, leading to a stabilization of the flow (Supplementary Discussion). On average it is up to 3 m s⁻¹ and found at approximately 25° S (Fig. 1a,b). Uplift also leads to a slight change in wind direction with a weakening of the easterly component and hence the wind becoming more parallel to the coast (Fig. 2). One factor contributing to this regional wind

intensification and pattern change is the elevated heating source over land in the present-day altitude simulation (HIGH). We find that zonal temperature gradients near the coast increase with uplift (Fig. 1c,d). Consequently, a deeper layer of baroclinity develops, which strengthens the along-coast winds, similar to the mechanism discussed for the California coastal jet involving thermal wind considerations[13,25]. Another cause for increased coastal baroclinity with mountain uplift is the barrier effect that leads to a mechanical blocking of onshore intrusion of higher momentum air, as was also demonstrated for the California coastal jet[25]. An important
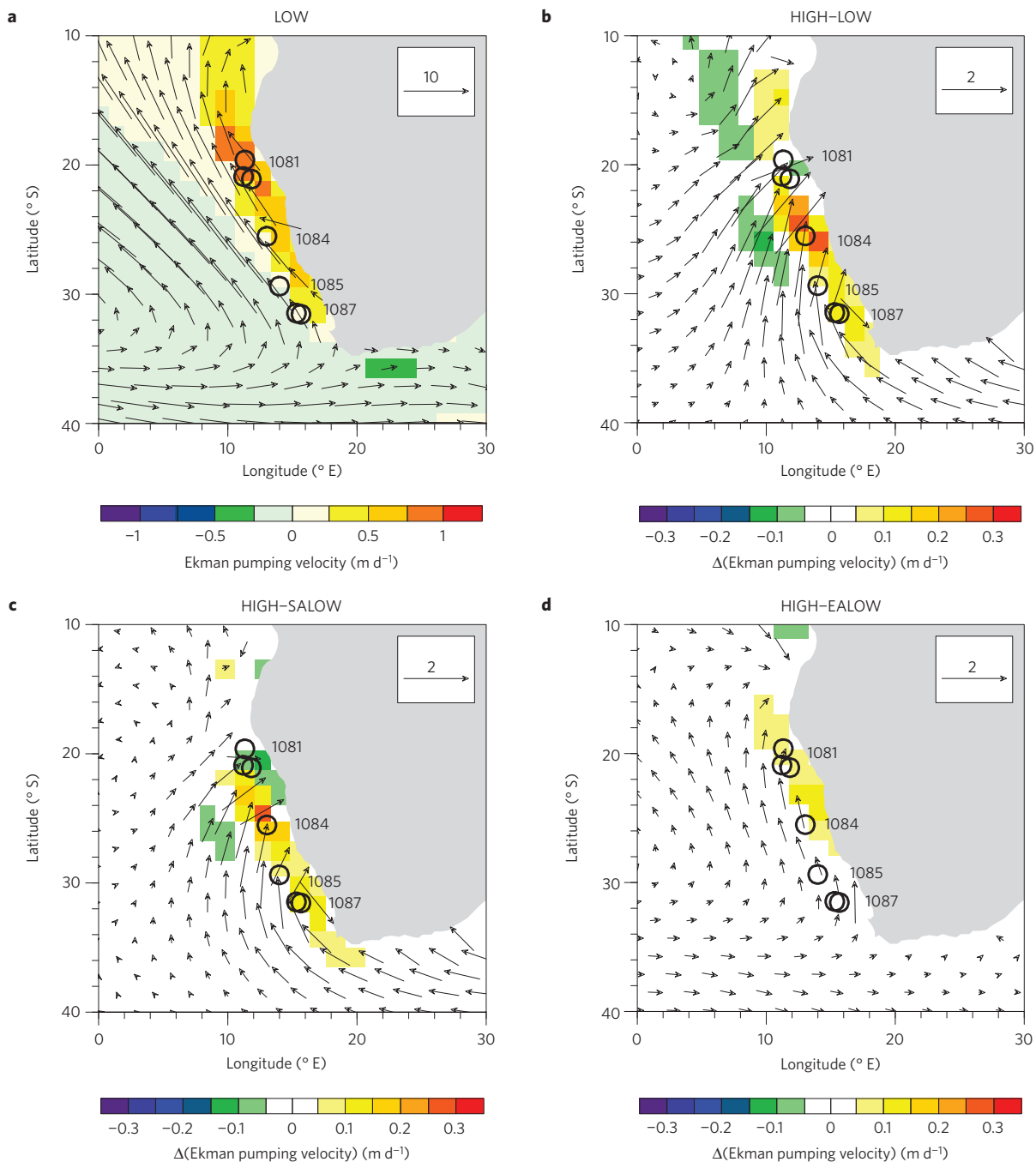
Figure 2 | Annual mean wind vectors at 1,000 hPa (m s⁻¹) and Ekman pumping velocity. a, For lowered African topography (LOW). **b**, Effect of eastern and southern African uplift (HIGH−LOW). **c**, Effect of southern African uplift (HIGH−SALOW). **d**, Effect of eastern African uplift (HIGH−EALOW); positive values indicate a strengthening of upwelling. Note the different scaling of the panels. The black circles and the associated numerical identifiers indicate the positions of Ocean Drilling Program sites that show Benguela upwelling intensification during the late Neogene.

effect of the increase in wind velocities and near-coastal wind stress for the surface ocean is an intensification of Ekman pumping in the Benguela region. Annual-mean Ekman pumping in our model experiment increases by up to 40–60% on eastern and southern African uplift, resulting in a substantial amplification of coastal upwelling (Fig. 2a,b). Considering the effects of East and southern African uplift separately, we demonstrate that the most important effect is due to uplift of southern Africa (Fig. 2c). However, uplift of eastern Africa also contributes to the intensification of coastal low-level winds and Ekman pumping, most likely through the thermal effect of elevated heating (Fig. 2d). The strengthened upwelling

of cooler waters from greater depths leads to a cooling of coastal surface ocean temperature, which in our experiment considering uplift of eastern and southern Africa reaches values of more than 3 °C, with a maximum cooling at around 60–80 m depth (Fig. 3a,b). The response of oceanic vertical velocity to uplift shows the largest anomalies between 30 and 180 m depth (Fig. 3c,d). Generally, maximum temperature anomalies are found where maximum vertical velocity anomalies coincide with large vertical temperature gradients. Considering the entire Benguela region, the strongest cooling due to uplift is, at the upper ocean levels, found near the coast. A strong agreement in the geographical and seasonal distribution
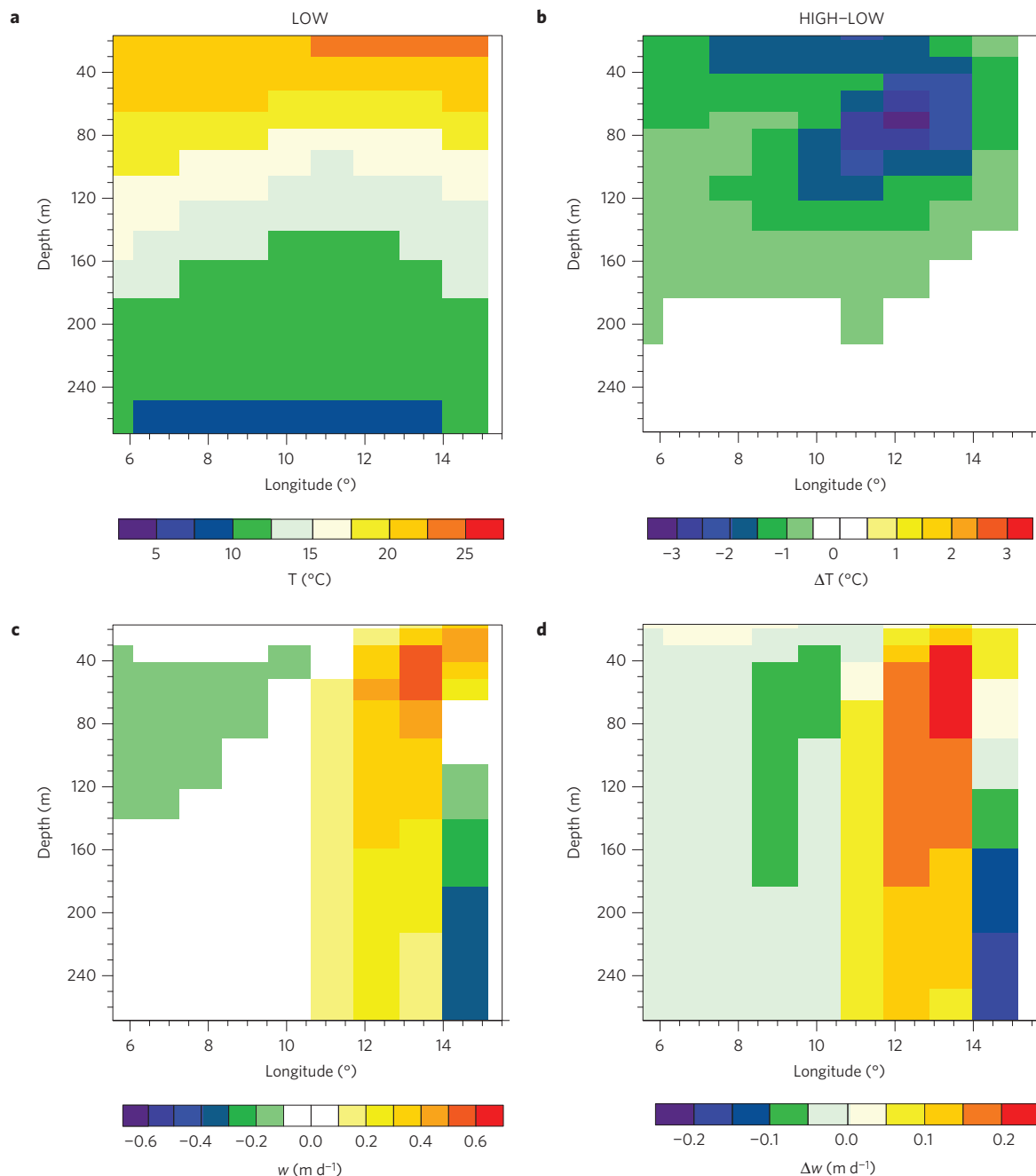
Figure 3 | Vertical cross-sections of annual mean ocean temperature and vertical velocity at 25° S, the latitude of the largest Ekman pumping anomaly.
a, Temperatures using lowered African topography (LOW). **b**, Temperature difference: effect of southern and eastern African uplift (HIGH–LOW).
c, Vertical velocity using lowered African topography (LOW). **d**, Vertical velocity difference: effect of southern and eastern African uplift (HIGH–LOW).

of the temperature and vertical velocity signals also indicates that the cooling is mostly determined by increased upwelling intensities (Supplementary Fig. 7). Performing a two-sided Student's t-test the response signal in upper ocean cooling turns out to be highly significant ($p < 0.01$; Fig. 4). The near-coastal cooling is transported to the northwest with the prevailing oceanic flow (which is also strengthened in the southern Benguela region; Fig. 5a,b). Feedback mechanisms through changing surface heat fluxes exist that could alter the cooling effect in the region (Fig. 5c–f). Sensible heat-flux change contributes to a heat loss in the upper ocean with a maximum of less than $20\,W\,m^{-2}$, due to stronger southwesterlies and turbulence. Net radiative heat flux into the ocean is reduced throughout the year owing to an increase in low-cloud coverage.

This is approximately balanced by the heat gain through a de-creasing latent heat flux from the ocean to the atmosphere (with maximum absolute values of more than $30\,W\,m^{-2}$ for both surface flux components).

Our experiments demonstrate that regional uplift of Africa induces increased wind stress and Ekman pumping, leading to a cooling of surface ocean temperatures in the Benguela region by up to $3\,°C$. Proxy reconstructions of Benguela Current sea surface temperature (SST) from middle Miocene to late Pliocene suggest a long-term cooling of about $8\,°C$ (ref. 2). CCSM3 is potentially biased towards underestimation of the strength and depth of coastal upwelling[26]. Comparing the capability to reproduce upwelling in our model set-up with a coarser resolved model simulation and with
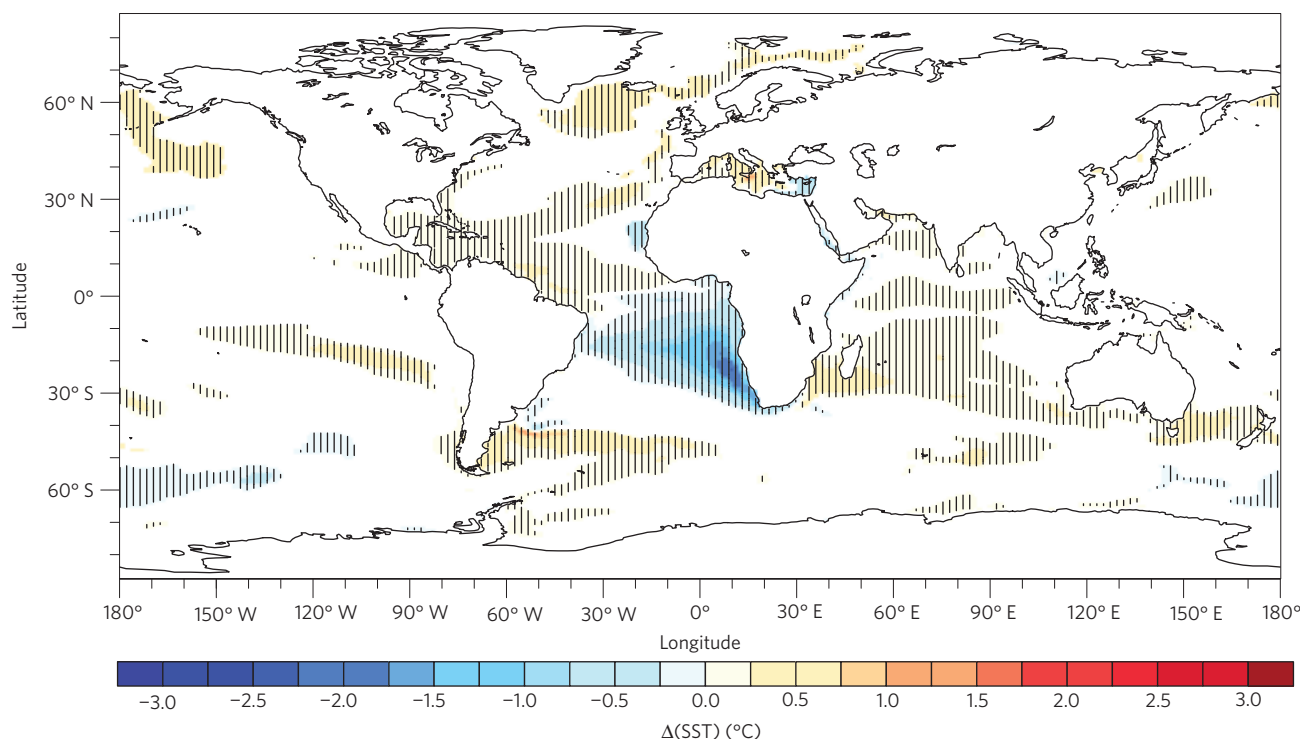
Figure 4 | Global change in annual mean sea surface temperature (SST) due to uplift of Africa. Regions of high significance ($p < 0.01$) are hatched.

highly resolved regional ocean model simulations demonstrates the ability to model upwelling with our set-up, but also the limitations in simulating the magnitude of upwelling (Methods and Supplementary Methods). Therefore, we assume that the magnitude of 2–3 °C of SST change derived from the CCSM3 modelling experiment represents a lower estimate of the expected signal caused by the uplift of African topography.

We compared our simulated response to uplift with the responses to the closure of the Panama Seaway in a CCSM3 study[9] and with the response to Antarctic glaciation in a slab ocean CESM1.0 run[11], as well as the response to a narrowing of the Indonesian Seaway in a simulation with the Kiel Climate Model[10]. All models were run at a lower resolution than our CCSM3 study; that is, the simulation of coastal upwelling is disabled. However, differences in wind stress and Ekman pumping can serve to identify potential responses in upwelling. Antarctic glaciation and the restriction of the Indonesian Throughflow both lead to a slight weakening of Ekman pumping velocities, whereas Panama closure causes a minor strengthening (Supplementary Figs 8 and 10). Nevertheless, both seaway closures act to reduce upper ocean temperatures owing to a redistribution of oceanic heat and/or a change in source region of water masses and hence lead to a slight surface cooling ($<1\,°C$) in the Benguela upwelling region. At least for the Panama experiment the cooling might be larger in the case of more realistic upwelling. However, there is no direct impact on wind stress and hence upwelling intensity (Supplementary Discussion). The timing of the tectonic events remains controversial, but a possible combination of these events could have acted in concert to intensify the cooling of the sea surface amplified by the positive feedback between the Benguela jet and upwelling. It seems unlikely that the sharp temperature decline in the northern Benguela upwelling region since the late Pliocene[3,4] can be solely connected to uplift of Africa despite increasing uplift rates in the Namibia region throughout the Pliocene[7]. SST reduction at that time is also observed in other upwelling systems. A major controlling factor was a reorganization of the global ocean inducing changes in the temperature and/or the depth of the thermocline[27].

However, an impact of uplift processes on upwelling intensification during the Pliocene cannot be excluded for other upwelling regions until similar studies are performed.

We suggest that African uplift was an important, and previously overlooked, factor in driving the late Neogene Benguela upwelling intensification and sea surface cooling recorded in proxy data[2]. Future studies refining model resolution or using limited area regional ocean (or coupled) models can potentially better quantify the effect of uplift on upwelling intensity and SST.

Methods

The simulations were performed with the National Center for Atmospheric Research (NCAR) CCSM3 (ref. 24). The model was run in a fully coupled mode, including the four components atmosphere, land, ocean, and sea ice. The atmospheric component (CAM3) and the land surface model were run at a horizontal resolution of ∼1.4° (T85); the atmosphere is discretized with 26 layers. The ocean (POP) and sea-ice (CSIM) models were run with a variable grid resolution of 1.125° in zonal direction and roughly 0.5° in meridional direction, with a refinement down to 0.3° at the Equator. The ocean model uses 40 levels in the vertical. A dynamic global vegetation model is coupled to the land model. To improve the simulation of vegetation cover, new parameterizations for canopy interception and soil evaporation have been implemented into the land component[28].

Like other global general circulation models, CCSM3 is not capable of reproducing the Atlantic equatorial cold tongue, but simulates an oceanic warm pool due to insufficient coastal currents and upwelling caused by a westerly wind bias[29], insufficient model resolution[29], and an insufficient representation of coastal atmosphere–ocean coupling[26]. Despite these known limitations, the model in the selected resolution turns out to be capable of reproducing coastal upwelling to some extent. Comparing the vertical velocity cross-section of the Benguela region (Fig. 3c) to a CCSM3 run in T31 resolution (∼3.75°) with an ocean zonal resolution of 3.6°, a variable meridional resolution down to ∼0.9° at the Equator and 25 levels in the vertical[9] (Supplementary Fig. 9c) shows that in the low-resolution run, no upwelling in the Benguela region is simulated at all. Supplementary Fig. 4 shows the seasonality of upwelling intensities in our control simulation (HIGH). In agreement with high-resolution modelling results[30], in our simulation the Lüderitz area shows only weak seasonality flanked by regions of spring and summer maximum to the south, and cells with a winter maximum to the north. The upwelling cells of the south (Cape Peninsula at ∼34° S together with Cape Columbine at ∼33° S and Namaqua at ∼30° S) seem to be
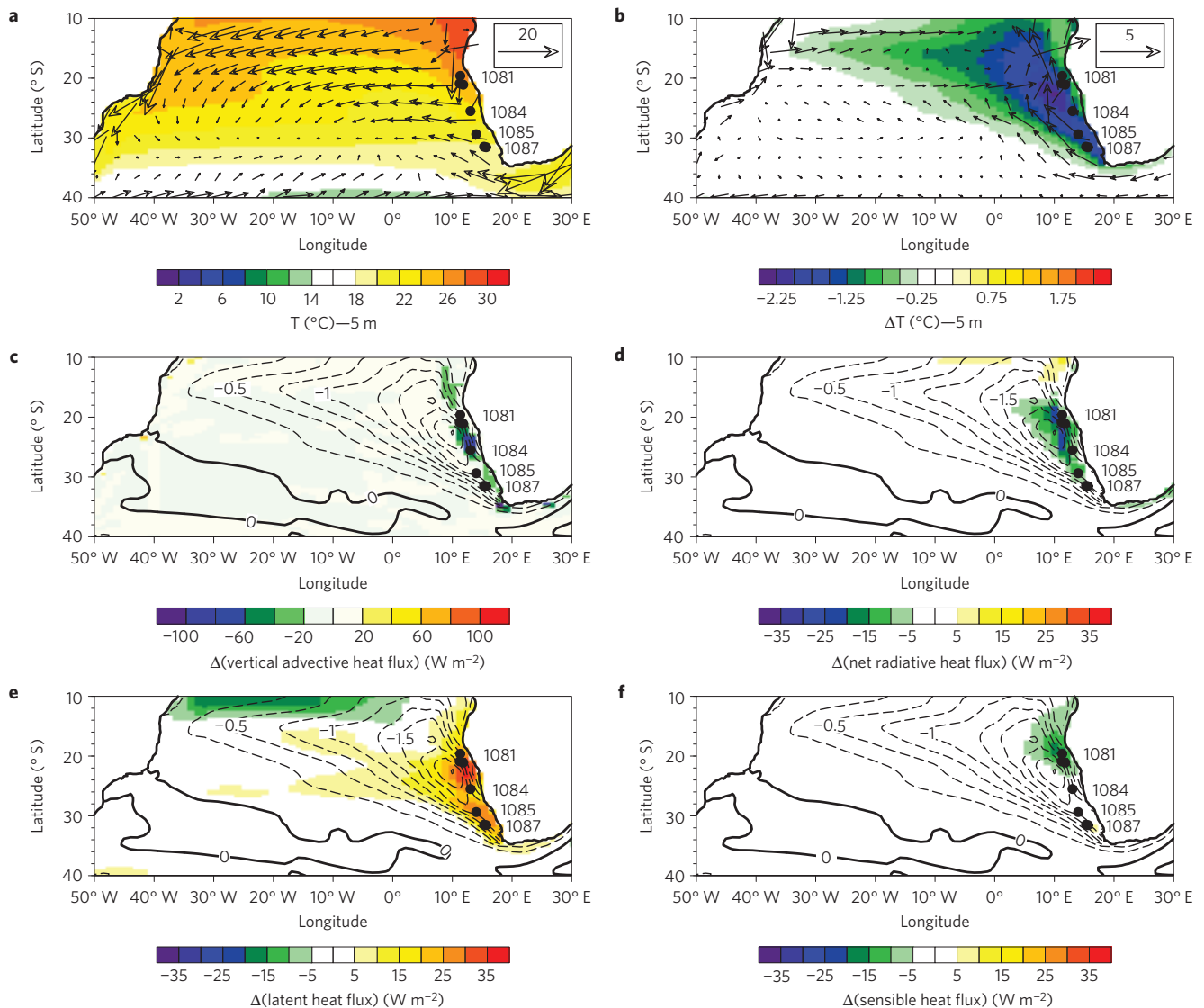
Figure 5 | Annual mean surface ocean temperature, flow and vertical heat flux responses to uplift of Africa; differences represent the effect of uplift (HIGH–LOW). a, Surface temperature (shaded) and horizontal velocity (cm s⁻¹) (LOW). **b**, Surface temperature (shaded) and horizontal velocity response. **c–f**, Contours: SST response. **c**, Vertical advective oceanic heat flux (upper 70 m; shaded). **d**, Net radiative heat flux (shaded). **e**, Latent heat flux (shaded). **f**, Sensible heat flux (shaded). Temperature contour interval: 0.25 °C. Positive values in **c–f** indicate a gain in oceanic heat content. The black dots and associated numerical identifiers indicate the positions of Ocean Drilling Program sites that show Benguela upwelling intensification during the late Neogene.

distinguishable, whereas the resolution is not high enough to resolve the northern cells, including Lüderitz, separately. Upwelling intensity never exceeds 1 m d⁻¹. Comparing the model outputs with more realistic values of (annual average) vertical velocities in the Benguela upwelling region, derived from high-resolution (9 km) regional ocean model simulations[30] of ∼7 m d⁻¹, shows the underestimation of upwelling in our model experiment. This leads us to assume an even larger magnitude of the upwelling intensification to be expected with uplift than what is indicated by our model experiment.

References

1. Hay, W. W. & Brock, J. C. Temporal variation in intensity of upwelling off southwest Africa. *Geol. Soc. London Spec. Publ.* **64,** 463–497 (1992).
2. Rommerskirchen, F., Condon, T., Mollenhauer, G., Dupont, L. & Schefuss, E. Miocene to Pliocene development of surface and subsurface temperatures in the Benguela Current system. *Paleoceanography* **26,** PA3216 (2011).
3. Rosell-Mele, A., Martinez-Garcia, A. & McClymont, E. L. Persistent warmth across the Benguela upwelling system during the Pliocene epoch. *Earth Planet. Sci. Lett.* **386,** 10–20 (2014).
4. Marlow, J. R., Lange, C. B., Wefer, G. & Rosell-Mele, A. Upwelling intensification as part of the Pliocene-Pleistocene climate transition. *Science* **290,** 2288–2291 (2000).
5. Diekmann, B., Falker, M. & Kuhn, G. Environmental history of the south-eastern South Atlantic since the Middle Miocene: Evidence from the sedimentological records of ODP Sites 1088 and 1092. *Sedimentology* **50,** 511–529 (2003).
6. Prange, M. & Schulz, M. A coastal upwelling seesaw in the Atlantic Ocean as a result of the closure of the Central American Seaway. *Geophys. Res. Lett.* **31,** L17207 (2004).
7. Roberts, G. G. & White, N. Estimating uplift rate histories from river profiles using African examples. *J. Geophys. Res.* **115,** B02406 (2010).
8. Chorowicz, J. The East African rift system. *J. Afr. Earth Sci.* **43,** 379–410 (2005).
9. Zhang, X. *et al.* Changes in equatorial Pacific thermocline depth in response to Panamanian seaway closure: Insights from a multi-model study. *Earth Planet. Sci. Lett.* **317,** 76–84 (2012).

10. Krebs, U., Park, W. & Schneider, B. Pliocene aridification of Australia caused by tectonically induced weakening of the Indonesian throughflow. *Palaeogeogr. Palaeoclimatol. Palaeoecol.* **309,** 111–117 (2011).
11. Goldner, A., Huber, M. & Caballero, R. Does Antarctic glaciation cool the world? *Clim. Past* **9,** 173–189 (2013).
12. Nicholson, S. E. A low-level jet along the Benguela coast, an integral part of the Benguela Current ecosystem. *Climatic Change* **99,** 613–624 (2010).
13. Burk, S. D. & Thompson, W. T. The summertime low-level jet and marine boundary layer structure along the California coast. *Mon. Weath. Rev.* **124,** 668–686 (1996).
14. Nyblade, A. A. & Robinson, S. W. The African Superswell. *Geophys. Res. Lett.* **21,** 765–768 (1994).
15. Seranne, M. & Anka, Z. South Atlantic continental margins of Africa: A comparison of the tectonic vs climate interplay on the evolution of equatorial west Africa and SW Africa margins. *J. Afr. Earth Sci.* **43,** 283–300 (2005).
16. Moucha, R. & Forte, A. M. Changes in African topography driven by mantle convection. *Nature Geosci.* **4,** 707–712 (2011).
17. Pik, R. East Africa on the rise. *Nature Geosci.* **4,** 660–661 (2011).
18. Erlanger, E. D., Granger, D. E. & Gibbon, R. J. Rock uplift rates in South Africa from isochron burial dating of fluvial and marine terraces. *Geology* **40,** 1019–1022 (2012).
19. Roberts, E. M. *et al.* Initiation of the western branch of the East African Rift coeval with the eastern branch. *Nature Geosci.* **5,** 289–294 (2012).
20. Sepulchre, P. *et al.* Tectonic uplift and Eastern Africa aridification. *Science* **313,** 1419–1423 (2006).
21. Al-Hajri, Y., White, N. & Fishwick, S. Scales of transient convective support beneath Africa. *Geology* **37,** 883–886 (2009).
22. Cohen, A. S., Soreghan, M. J. & Scholz, C. A. Estimating the age of formation of lakes — an example from Lake Tanganyika, East-African Rift system. *Geology* **21,** 511–514 (1993).
23. Sepulchre, P., Sloan, L. C., Snyder, M. & Fiechter, J. Impacts of Andean uplift on the Humboldt Current system: A climate model sensitivity study. *Paleoceanography* **24,** PA4215 (2009).
24. Collins, W. D. *et al.* The community climate system model version 3 (CCSM3). *J. Clim.* **19,** 2122–2143 (2006).
25. Holt, T. R. Mesoscale forcing of a boundary layer jet along the California coast. *J. Geophys. Res.* **101,** 4235–4254 (1996).
26. Large, W. G. & Danabasoglu, G. Attribution and impacts of upper-ocean biases in CCSM3. *J. Clim.* **19,** 2325–2346 (2006).
27. Dekens, P. S., Ravelo, A. C. & McCarthy, M. D. Warm upwelling regions in the Pliocene warm period. *Paleoceanography* **22,** PA3211 (2007).
28. Oleson, K. W. *et al.* Improvements to the Community Land Model and their impact on the hydrological cycle. *J. Geophys. Res.* **113,** G01021 (2008).
29. Grodsky, S. A., Carton, J. A., Nigam, S. & Okumura, Y. M. Tropical Atlantic biases in CCSM4. *J. Clim.* **25,** 3684–3701 (2012).
30. Veitch, J., Penven, P. & Shillington, F. Modeling equilibrium dynamics of the Benguela Current system. *J. Phys. Oceanogr.* **40,** 1942–1964 (2010).

Author contributions

M.P. and M.S. developed the project. G.J., M.P. and M.S. interpreted the model results and wrote the paper. G.J. performed the model simulations, analysed the model results and created the figures.

Additional information

Supplementary information is available in the online version of the paper. Reprints and permissions information is available online at www.nature.com/reprints. Correspondence and requests for materials should be addressed to G.J.

Competing financial interests

The authors declare no competing financial interests.

747

Uplift of Africa as a potential cause for Neogene intensification of the Benguela upwelling system

Gerlinde Jung, Matthias Prange, Michael Schulz

MARUM - Center for Marine Environmental Sciences and Faculty of Geosciences, University of Bremen, 28334 Bremen, Germany.

Correspondence to: G. Jung (gjung@marum.de)

I) Supplementary Methods

## Simulation setup, spin up and output analysis

The following experiments were performed to investigate the impact of uplift of Africa on Benguela upwelling:

⇨ A control simulation (HIGH) using present-day topography (as described in detail in the following paragraph).

⇨ A simulation identical to HIGH, except for a lowered eastern and southern African topography (LOW), to half of the present-day level.

Additionally, the following two experiments were performed to disentangle the effects of uplift of eastern and southern Africa and to be able to describe processes that drive upwelling intensification connected to uplift of both regions separately:

⇨ A simulation identical to HIGH, except for a lowered southern African topography (SALOW), to half of the present-day level.

⇨ A simulation identical to HIGH, except for a lowered eastern African topography (EALOW), to half of the present-day level.

Supplementary Fig. 1 shows the model topographies of all performed experiments.

2
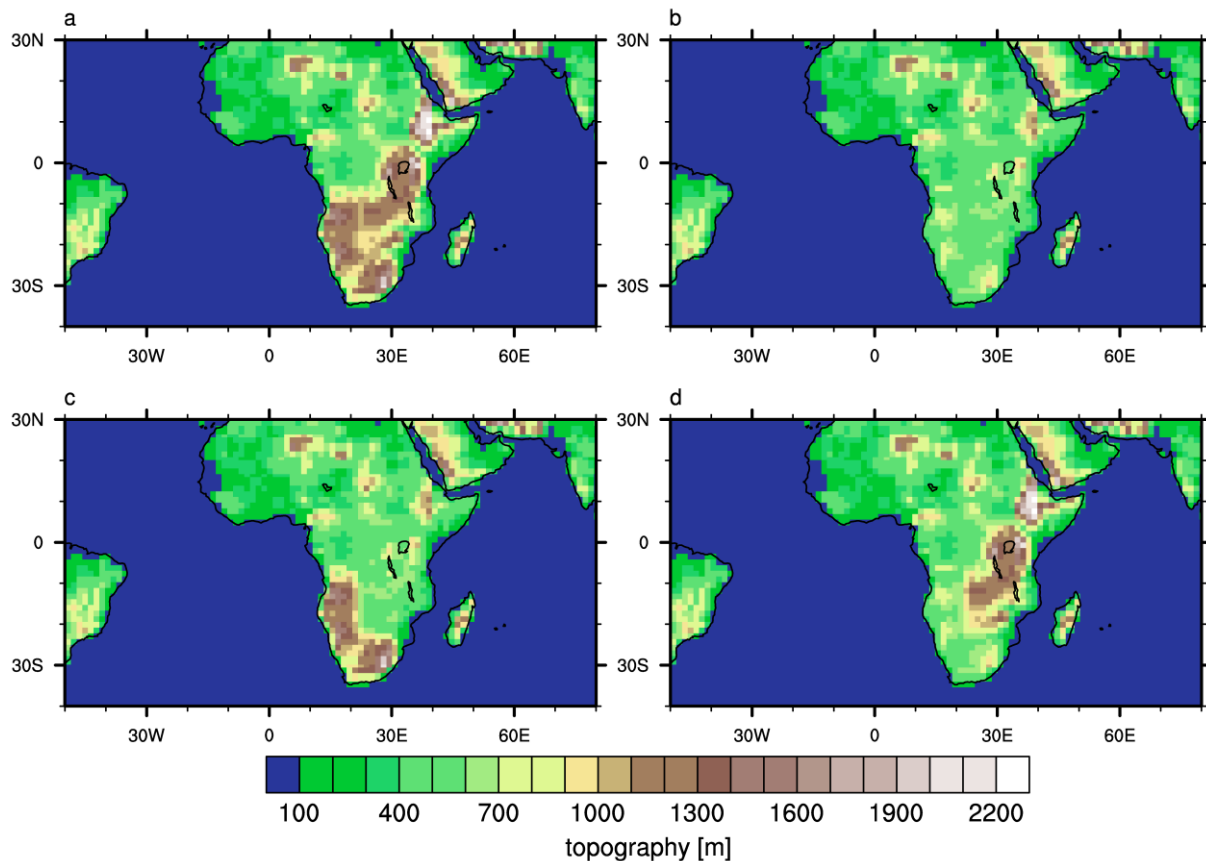
Supplementary Figure 1 | Topography of the model experiments. **a**, Present-day altitude (HIGH). **b**, Half the present-day altitude in eastern and southern Africa (LOW). **c**, Half the present-day altitude in eastern Africa (EALOW). **d**, Half the present-day altitude in southern Africa (SALOW).

The following boundary conditions were chosen for the control run (HIGH):

1) Greenhouse gas and ozone concentrations, sulphate and carbonaceous aerosol distributions follow the guidelines for pre-industrial simulations formulated within the Paleoclimate Modelling Intercomparison Project, Phase 2 (PMIP-2)[1].

2) The effect of dust aerosols on radiative transfer was set to zero. Soil texture and colour were adapted to be loam in the Sahara, to represent the pre-desert conditions in the Miocene/early Pliocene period.

3) The orbital parameters were changed to represent average values over a longer

3

period (2-10 Ma) with an eccentricity of 0.027 and an obliquity of 23.25°. The perihelion was set to autumn (359.47°) to avoid extreme insolation forcing.

Compared to a pure pre-industrial run that was also performed, our control simulation is characterized by stronger (weaker) insolation in the northern hemisphere in summer (winter), which leads to an increase in seasonality, most pronounced in the northern hemisphere.

The control run was started from a spun-up preindustrial simulation of 500 years obtained from the National Center for Atmospheric Research (NCAR) and run for another 600 years. The experiments were branched off from the control run at year 301 and run for another 300 years. Averages over the last 100 years of each experiment were taken for analysis of the results.

Supplementary Fig. 2 demonstrates that the oceanic surface layer is in equilibrium after 300 years of spin-up, whereas the upper 500 m of the water column still needs more than another ~200 years to reach equilibrium, even though after 300 years of spin-up also here the trend to lower temperatures is weak. Equilibration of the deep ocean is not essential for our study because the considered upwelling processes are restricted to the topmost ocean layers (~200 m). The vertical velocity in the upper ocean in the Benguela region does not show any significant trend after the spin-up period either, as demonstrated in Supplementary Fig. 3.

Averages over the last 100 years of each experiment were taken for analysis of the results. All figures shown in this paper are based on these 100 year means.
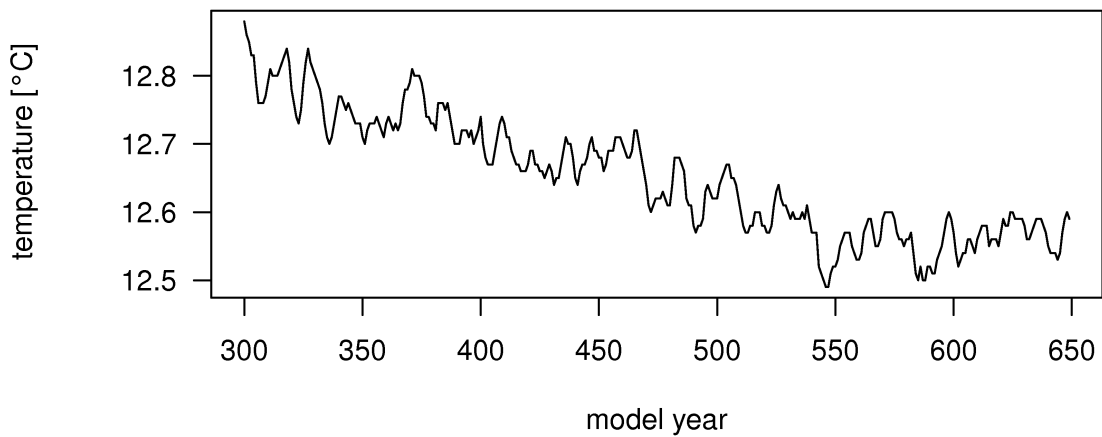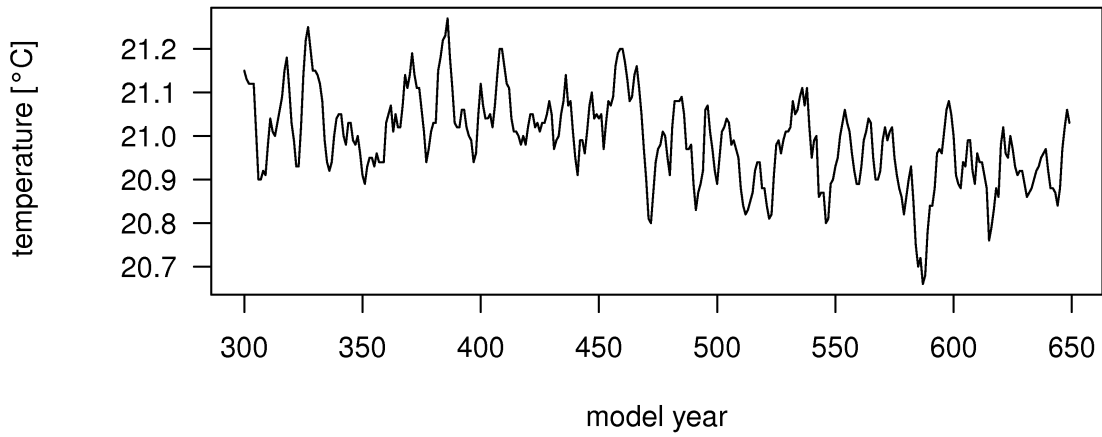
Supplementary Figure 2 | Spin-up of the upper ocean: averaged ocean temperature [°C] time series (HIGH) in the South-East Atlantic (0 - 40°S, 40°W - 22°E). Note that this simulation was extended by another 50 years for the purpose of demonstrating equilibration of the temperatures. Top: upper ~100 m; bottom: upper ~500 m.

5
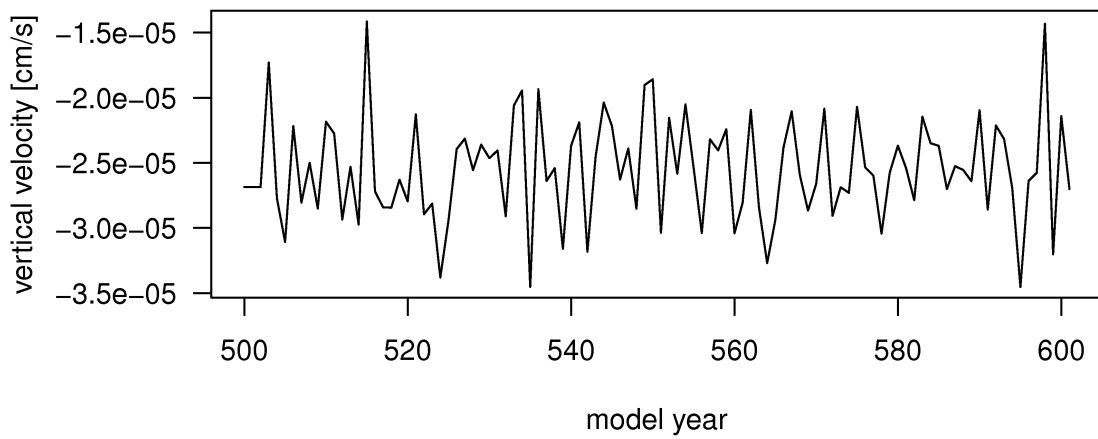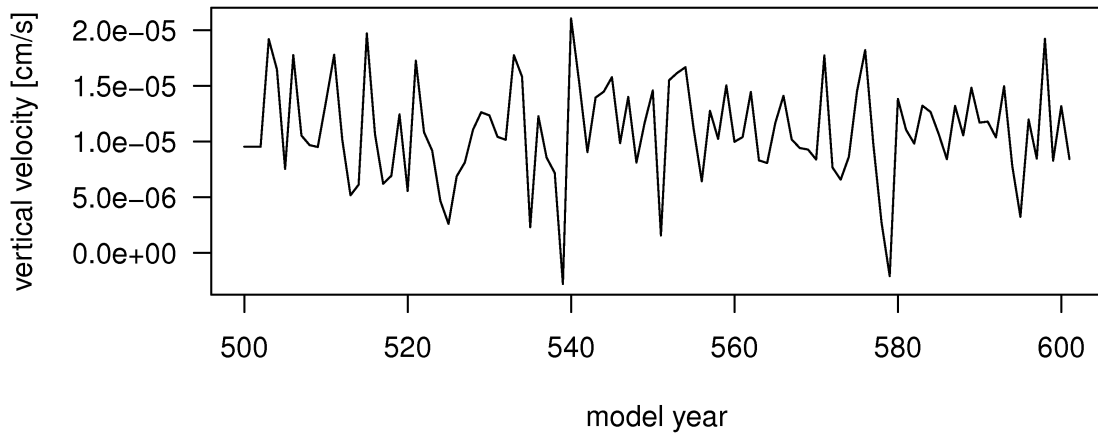
Supplementary Figure 3 | Spin-up of the upper ocean: averaged ocean vertical velocity [cm/s] time series for the last 100 model years (HIGH) in the Benguela Current and Upwelling region (0 - 40°S, 7°W - 22°E). Top: upper ~100 m; bottom: upper ~500 m.

6

Capability of the model to reproduce coastal upwelling

Supplementary Fig. 4 demonstrates the capability of the model to simulate seasonally varying upwelling intensities in the Benguela region, as discussed in more detail in the Methods section of the main text.
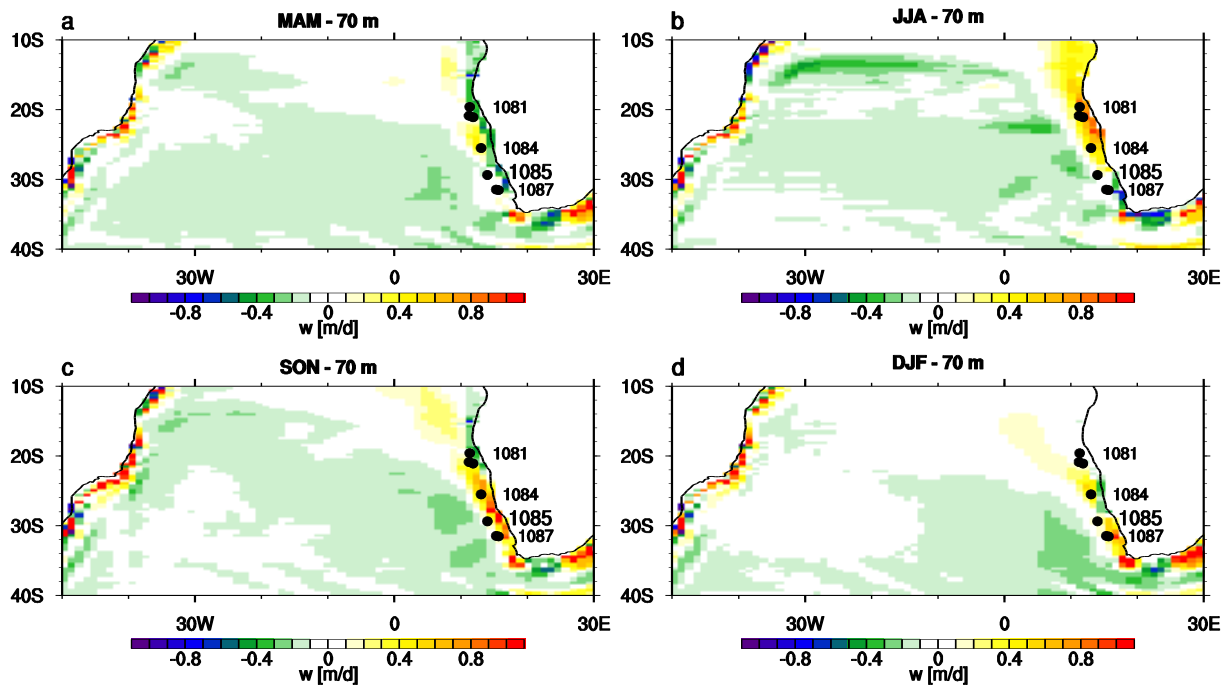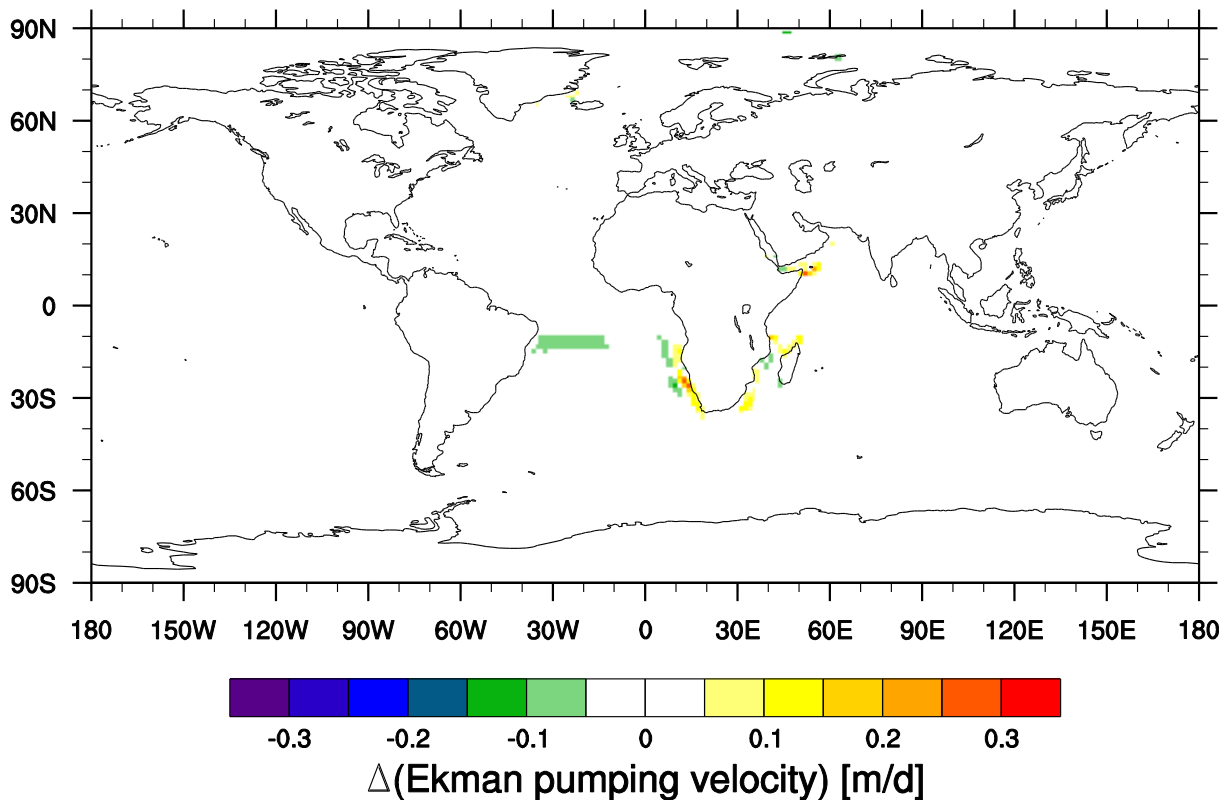

Supplementary Figure 4 | Seasonal variability (HIGH) in vertical velocity (shaded) at 70 m depth. The black dots indicate the positions of ODP sites that show Benguela upwelling intensification during the late Neogene[2-5]. Site 1085 is highlighted because it is the only record that covers the entire period from the mid-Miocene to the Pliocene.

7

II) Supplementary Discussion

Significance of the model results

Considering the global distribution of the response in Ekman pumping clearly shows that the signal is regionally limited with changes occurring around Africa being strongest and most extended in the Benguela region (Supplementary Fig. 5)

$\triangle$(Ekman pumping velocity) [m/d]

Supplementary Figure 5 | Global change in Ekman pumping velocity due to uplift of eastern and southern Africa, demonstrating the significance of the response in the Benguela region.

Seasonal variations: Benguela Jet, upwelling intensity and temperature change

The seasonal variability in the model's response to uplift shows that the strengthening of the Benguela Jet is evident throughout the year, but most pronounced in the austral autumn and winter seasons, when the jet itself is weakest

8

(Supplementary Fig. 6). This indicates a stabilization of the winds along the coast, which is an important prerequisite for intense oceanic upwelling to develop.

The seasonal and geographical accordance of temperature changes and vertical velocity changes (Supplementary Fig. 7) shows the strong relationship of the two variables, confirming the causal relationship.
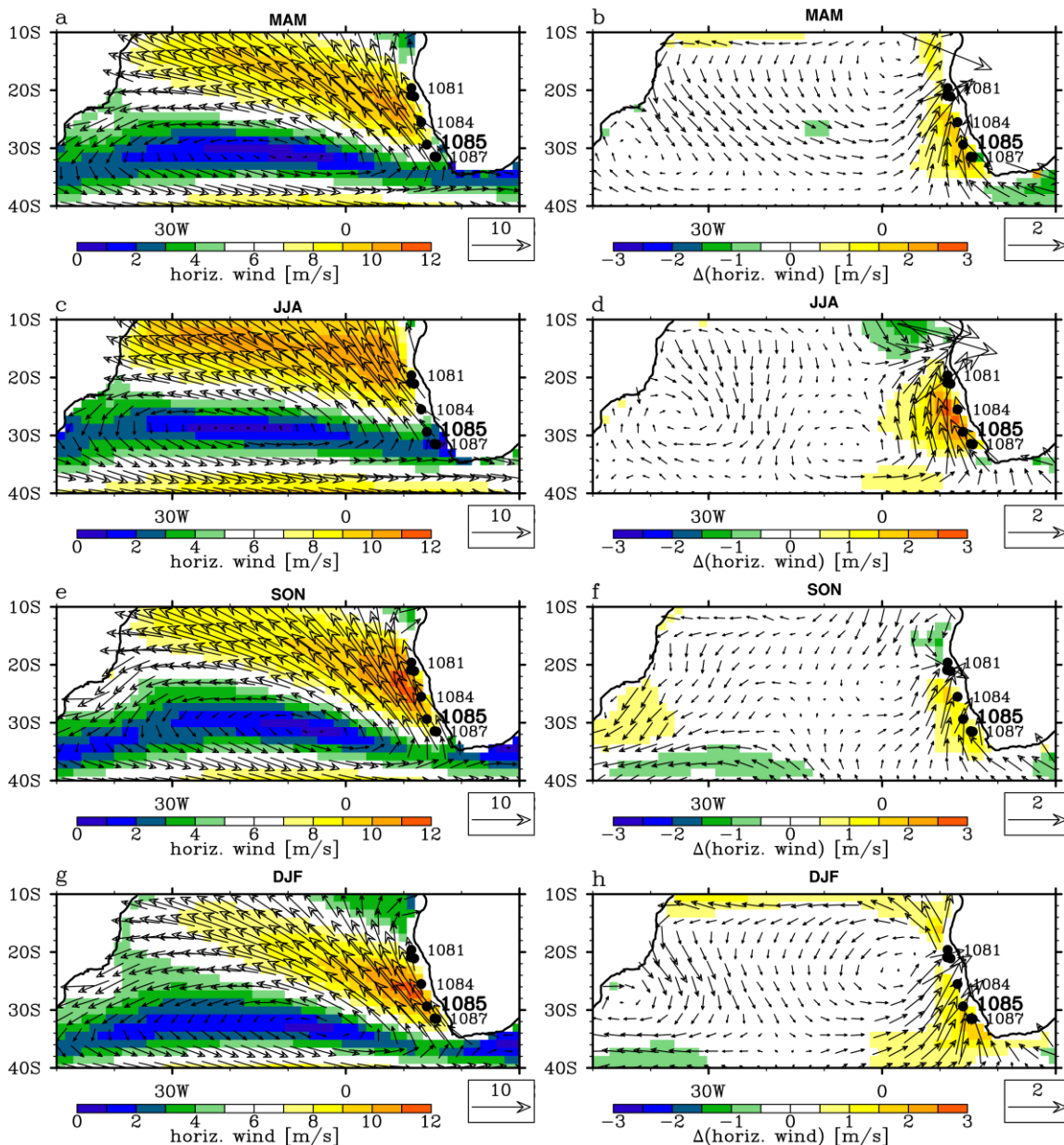
Supplementary Figure 6 | Seasonal variability of horizontal wind at 925 hPa (a,c,e,g) and respective changes with uplift (difference: HIGH − LOW) (b,d,f,h). The black dots indicate the positions of ODP sites that show Benguela upwelling intensification during the late Neogene[2-5]. Site 1085 is highlighted because it is the only record that covers the entire period from the mid-Miocene to the Pliocene.

9
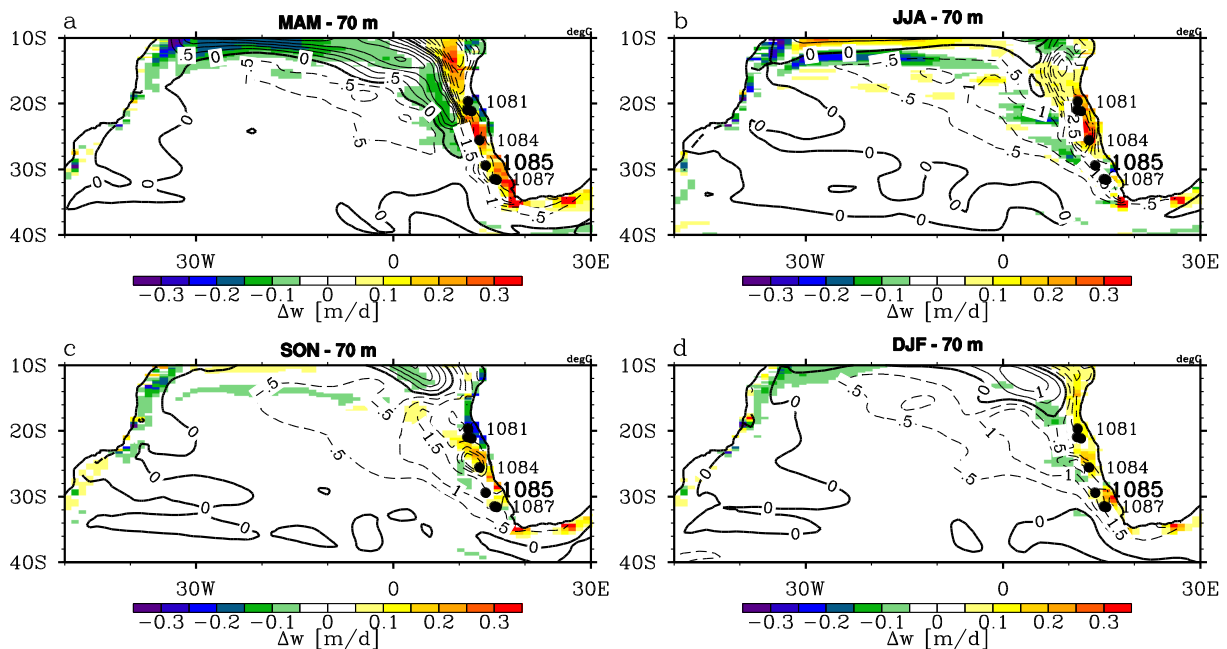
Supplementary Figure 7 | Seasonal variability of difference (HIGH – LOW) in ocean temperature (contours) and vertical velocity (shaded) at 70 m depth. The temperature contour interval is 0.5°C. The black dots indicate the positions of ODP sites that show Benguela upwelling intensification during the late Neogene[2-5]. Site 1085 is highlighted because it is the only record that covers the entire period from the mid-Miocene to the Pliocene.

Alternative hypotheses

Several hypotheses have been proposed to explain upwelling intensification and upper ocean cooling in the Benguela region during the late Neogene.

It has been suggested that, following the intensified Antarctic glaciation from Mid-Miocene onwards, the increasing unipolar glaciation caused a northward displacement of the subtropical South Atlantic high pressure system and the Intertropical Convergence Zone along with a strengthening of the trade winds due to an increased meridional temperature gradient[6,7]. A change in ocean stratification[6] and/or a strengthening of the subtropical high pressure cell, and hence the trade winds, caused by a cooling of the South Atlantic in response to the Pliocene closure of the Central American Seaway[8], were also discussed as mechanisms for the Benguela upwelling intensification. However, recent geochronological and

10

geochemical data together with numerical modelling suggest an earlier restriction of the seaway (~15 Ma) long before the Pliocene[9]. Also the narrowing of the Indonesian seaway has been proposed as mechanism explaining late Pliocene to Pleistocene intensification of the meridional SST gradient and cooling in the Benguela upwelling region, through cooling and shoaling of the eastern Indian Ocean thermocline and a transport of the cooling signal to the Benguela region via the Agulhas leakage[10,11].

In comparison to an earlier study simulating the effect of a Panama closure[8] with a climate model of intermediate complexity, our model results show an increase in wind stress due to uplift that is four to ten times larger in the Benguela upwelling region. Additionally, we compared the simulated response to uplift with the response to the closure of the Panama Seaway in a CCSM3 study[12] and to Antarctic glaciation in a slab ocean CESM1.0 run[13], as well as to a narrowing of the Indonesian seaway in a KCM simulation[14] (Supplementary Figs. 8-11). For the Antarctic glaciation experiment, the induced changes in wind stress and Ekman pumping are not only very small, but indicate a weakening of upwelling rather than the expected strengthening (Supplementary Fig. 8c). A recent study, simulating the global effect of Antarctic glaciation in a Mid-Miocene model setup also showed a surface air temperature warming in the Benguela region[15]. For the Central American Seaway closure various model experiments indicate an upper ocean cooling in the South Atlantic due to strengthened Atlantic Meridional Overturning Circulation[12]. In the case of the low-resolution CCSM3 experiment[12] we see only a minor strengthening of Ekman pumping velocities (Supplementary Fig. 8b), but a cooling that shows an increase with depth (Supplementary Fig. 9). Therefore, an additional SST reduction, when seaway closure and African uplift act in concert, seems possible in case of realistic vertical velocities. The restriction of the Indonesian Throughflow, in a low-resolution modelling study with the Kiel Climate Model[14], also leads to a weak SST cooling (< 1°C) of the Southern Atlantic despite a slight decrease in Ekman pumping (Supplementary Fig. 10a). However, the cooling is restricted to the surface ocean layers (Supplementary Fig. 10b), hence no larger decrease in sea surface temperature is expected in case of more realistic upwelling conditions. Supplementary Fig. 11 indicates that the cooling in the Benguela region might not be due to a transport of a cooling signal from the eastern Indian Ocean as proposed earlier[11]. From surface wind forcing we would expect rather a weakening of the

11

Agulhas leakage caused by an intensification and/or a northward displacement of the maximum in Southern Hemisphere Westerlies that potentially alters the sources of waters entering the Benguela upwelling region. A model resolution of at least 0.1° would however be necessary for a realistic simulation of the Agulhas leakage[16].

The comparison of our model results with the alternative experiments shows that uplift plays an important role in creating upwelling-favorable conditions in terms of wind stress in the Benguela region that hence lead to a significant upper ocean cooling.
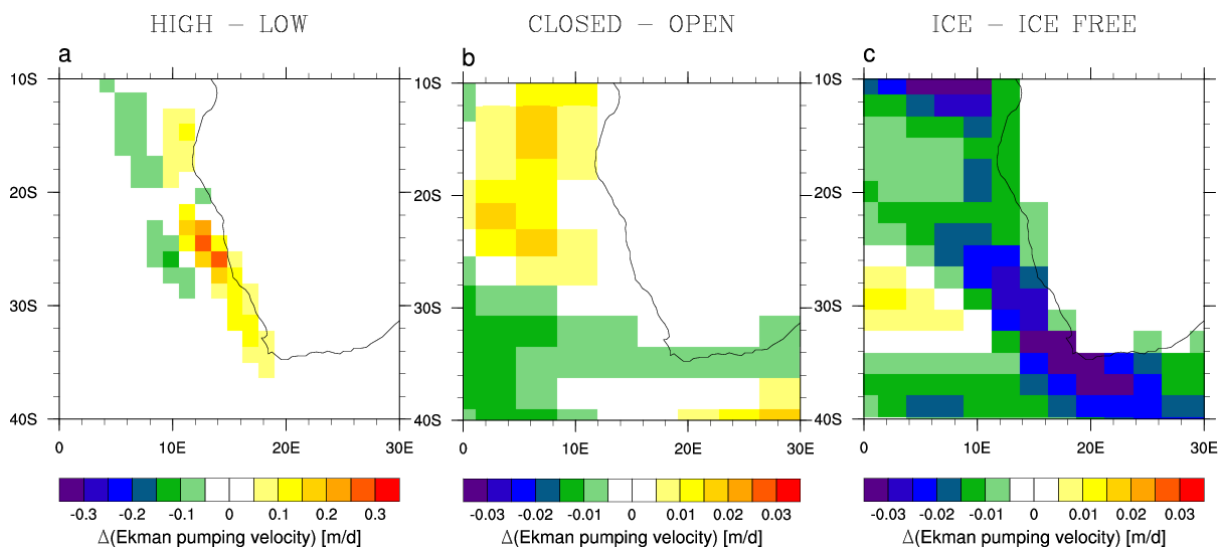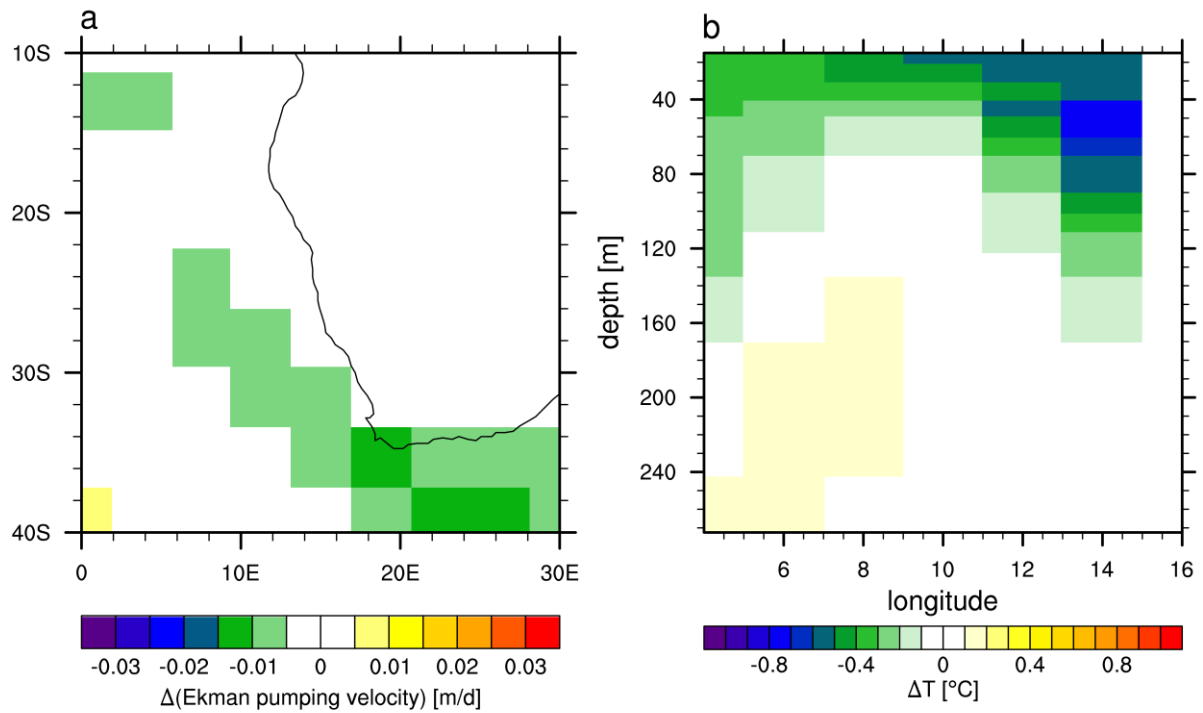

Supplementary Figure 8 | Change in Ekman pumping velocity (long-term annual mean). a, Due to uplift, as simulated in the present study (CCSM3, resolution: T85). **b,** Due to the closure of the Central American seaway (CCSM3, resolution: T31[12]). **c,** Due to glaciation of Antarctica (CESM1.0, resolution: 2x2.5°, slab ocean[13]). Note different scaling of panels.
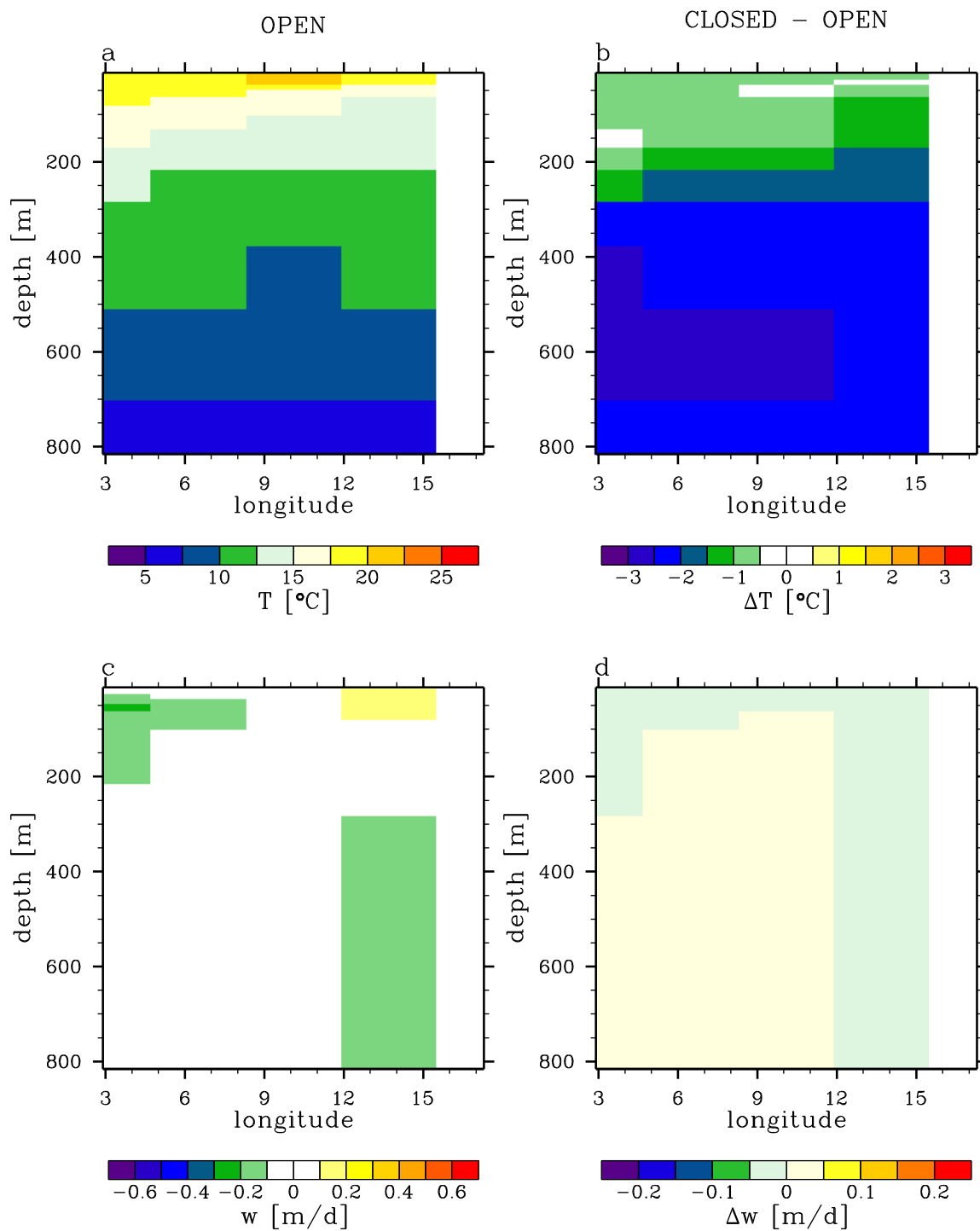
Supplementary Figure 9 | CCSM3/T31 run[12]: vertical cross-sections of annual mean ocean temperature and vertical velocity at 25°S.

a, Temperatures with opened Panama Seaway (OPEN). **b,** Temperature difference with respect to closed Panama Seaway (CLOSED – OPEN). **c,** Vertical velocity with opened Panama Seaway (OPEN). **d,** Vertical velocity difference (CLOSED – OPEN).

Supplementary Figure 10 | Response to Indonesian Throughflow restriction (CLOSED - OPEN). Model experiment using the Kiel Climate Model (KCM), resolution: T31[14]. **a,** Change in Ekman pumping velocity. **b,** Vertical cross-sections of annual mean ocean temperature change at 25°S.
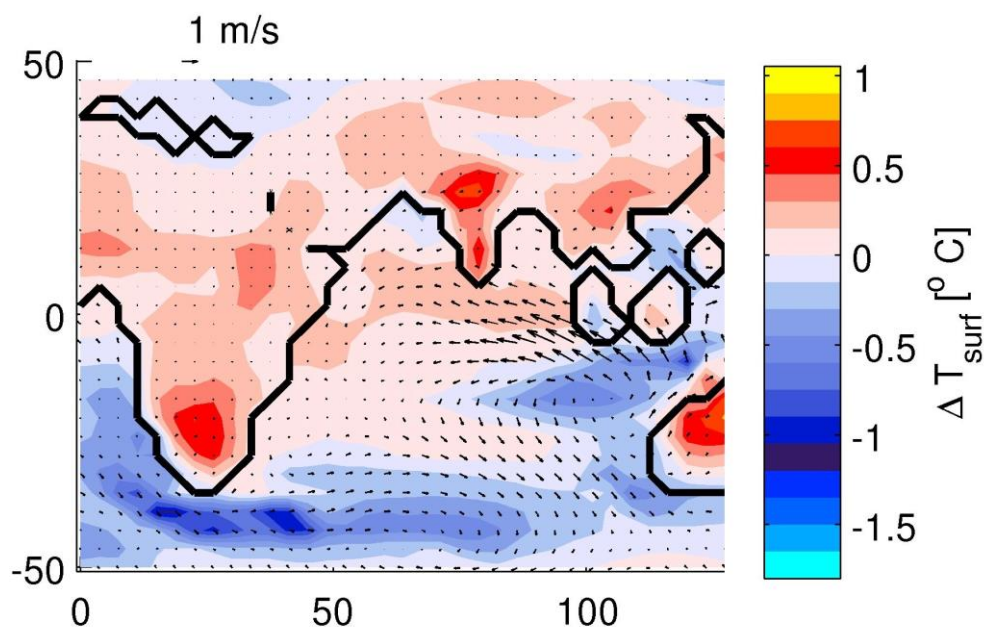
Supplementary Figure 11 | Change in surface wind and SST due to a restriction of the Indonesian Throughflow. Model experiment using the Kiel Climate Model (KCM), resolution: T31[14]. Figure (modified) by courtesy of Uta Krebs-Kanzow, AWI.

References

1   Braconnot, P. *et al.* Results of PMIP2 coupled simulations of the Mid-Holocene and Last Glacial Maximum - Part 1: experiments and large-scale features. *Climate of the Past* **3**, 261-277 (2007).

2   Gorgas, T. J. & Wilkens, R. H. Sedimentation rates off SW Africa since the late Miocene deciphered from spectral analyses of borehole and GRA bulk density profiles: ODP Sites 1081-1084. *Mar Geol* **180**, 29-47 (2002).

3   Rommerskirchen, F., Condon, T., Mollenhauer, G., Dupont, L. & Schefuss, E. Miocene to Pliocene development of surface and subsurface temperatures in the Benguela Current system. *Paleoceanography* **26**, PA3216 (2011).

4   Marlow, J. R., Lange, C. B., Wefer, G. & Rosell-Mele, A. Upwelling intensification as part of the Pliocene-Pleistocene climate transition. *Science* **290**, 2288-2291 (2000).

5   Diester-Haass, L., Meyers, P. A. & Bickert, T. Carbonate crash and biogenic bloom in the late Miocene: Evidence from ODP Sites 1085, 1086, and 1087 in the Cape Basin, southeast Atlantic Ocean. *Paleoceanography* **19**, PA1007 (2004).

6   Hay, W. W. & Brock, J. C. Temporal variation in intensity of upwelling off southwest Africa. *Geological Society, London, Special Publications* **64**, 463-497 (1992).

7   Heinrich, S., Zonneveld, K. A. F., Bickert, T. & Willems, H. The Benguela upwelling related to the Miocene cooling events and the development of the Antarctic Circumpolar Current: Evidence from calcareous dinoflagellate cysts. *Paleoceanography* **26**, PA3209 (2011).

8   Prange, M. & Schulz, M. A coastal upwelling seesaw in the Atlantic Ocean as a result of the closure of the Central American Seaway. *Geophysical Research Letters* **31**, L17207 (2004).

9   Sepulchre, P. *et al.* Consequences of shoaling of the Central American Seaway determined from modeling Nd isotopes. *Paleoceanography* **29**, 176-189 (2014).

10   Rosell-Mele, A., Martinez-Garcia, A. & McClymont, E. L. Persistent warmth across the Benguela upwelling system during the Pliocene epoch. *Earth and Planetary Science Letters* **386**, 10-20 (2014).

11   Karas, C. *et al.* Mid-Pliocene climate change amplified by a switch in Indonesian subsurface throughflow. *Nature Geoscience* **2**, 434-438 (2009).

12   Zhang, X. *et al.* Changes in equatorial Pacific thermocline depth in response to Panamanian seaway closure: Insights from a multi-model study. *Earth and Planetary Science Letters* **317**, 76-84 (2012).

13   Goldner, A., Huber, M. & Caballero, R. Does Antarctic glaciation cool the world? *Climate of the Past* **9**, 173-189 (2013).

14   Krebs, U., Park, W. & Schneider, B. Pliocene aridification of Australia caused by tectonically induced weakening of the Indonesian throughflow. *Palaeogeography, Palaeoclimatology, Palaeoecology* **309**, 111-117 (2011).

15   Knorr, G. & Lohmann, G. Climate warming during Antarctic ice sheet expansion at the Middle Miocene transition. *Nature Geoscience* **7**, 376-381 (2014).

16   Beal, L. M., De Ruijter, W. P. M., Biastoch, A., Zahn, R. & 136, S. W. I. W. G. On the role of the Agulhas system in ocean circulation and climate. *Nature* **472**, 429-436 (2011).